

Kinetics of stimulated polariton scattering in planar microcavities: Evidence for a dynamically self-organized optical parametric oscillator

A. A. Demenev,¹ A. A. Shchekin,¹ A. V. Larionov,¹ S. S. Gavrilov,^{1,2}
V. D. Kulakovskii,¹ N. A. Gippius,^{2,3} and S. G. Tikhodeev^{2,3}

¹*Institute of Solid State Physics RAS, Chernogolovka, 142432 Russia*

²*A. M. Prokhorov General Physics Institute RAS, Moscow, 119991 Russia*

³*LASMEA, UMR 6602 CNRS, Université Blaise Pascal, Aubière, France*

(Dated: November 26, 2007)

We demonstrate for the first time the strong temporal hysteresis effects in the kinetics of the pumped and scattered polariton populations in a planar semiconductor microcavity under a nano-second-long pulsed resonant (by frequency and angle) excitation above the lower polariton branch. The hysteresis effects are explained in the model of multi-mode scattering when the bistability of the nonlinear pumped polariton is accompanied by the explosive growth of the scattered polaritons population. Subsequent self-organization process in the nonlinear polariton system results in a new — dynamically self-organized — type of optical parametric oscillator.

PACS numbers: 71.36.+c, 42.65.Pc, 42.55.Sa

A giant stimulated polariton-polariton scattering is one of the most striking features in the optical response of planar microcavities (MCs). The scattering was firstly observed in GaAs-based MCs with InGaAs quantum wells (QWs) in the active layer under a cw excitation at wave-vector \mathbf{k}_p close to the inflection point of lower polariton (LP) branch $\omega_{LP}(\mathbf{k})$, when the scattering exhibits an unusually low (smaller than 400 W/cm²) threshold [1, 2, 3]. Specifically, such excitation results in the strong parametric scattering into states positioned approximately on $\omega_{LP}(\mathbf{k})$ with $\mathbf{k}_s = 0$ and $\mathbf{k}_i = 2\mathbf{k}_p$, called signal and idler, respectively. The effect was theoretically described in terms of four-wave mixing or parametric scattering [4, 5, 6]. Subsequent studies [7, 8, 9] have shown that the shift of the excitation from the inflection point of the LP dispersion is not followed by the corresponding shift of the stimulated scattering along the LP branch characteristic for the four wave mixing. Instead, the scattering goes on to the same states with $\mathbf{k} \sim 0$ and $\sim 2\mathbf{k}_p$. The energy conservation is then fulfilled by the shift of the signal and the idler much above the LP branch.

The stability analysis of the single macro-occupied pump mode as well as numerical simulations of the polariton scattering indicate [9, 10, 11, 12] that such unusual behavior can result from the interplay between two instabilities in the resonantly excited MC: bistability of the pumped polariton mode intensity with respect to the external pump, and its parametric instability with respect to the decay into multiple scattered polaritons in a wide range of \mathbf{k} .

The single-mode optical bistability in MC for pumping at $\mathbf{k}_p = 0$ has been observed and explained theoretically within one-mode optical parametric oscillator (OPO) model [13]. The bistability of the scattered signal at pumping near inflection point was also found and

explained within three-mode OPO model [14].

Different possible regimes of the above-threshold OPO have been analyzed theoretically within the three-mode approximation [15, 16]. However three-mode OPO model cannot determine the signal and idler wave vectors $\mathbf{k}_{s,i}$ which are selected by the parametric process above threshold. In the system with a specific dispersion (containing an inflection point), the interplay between the pump single mode bistability and its multi-mode parametric instability can result in a regime where essentially multi-mode coupling between the ensemble of lower polaritons plays the decisive role in the formation of the signal and idler [9, 11, 17]. We will refer to this model as a *dynamically self-organized (DSO) OPO*.

Dramatic change of LP scattering pattern from the figure-of-eight shape corresponding to spontaneous regime at lower pump intensity [4, 18] to that directed along $\mathbf{k} \sim 0$ and $\sim 2\mathbf{k}_p$ for pump powers above the parametric scattering threshold observed recently [19] supports the DSO OPO model. However, the direct evidence of multi-mode self-organized nature of the scattering demands the study of the LP system dynamics. The previous time-resolved studies of the LP dynamics under ps-long excitation pulses [18] have revealed a well pronounced figure-of-eight distribution of the final LP scattering states in low excitation regime, but only a small narrowing of the LP momentum distribution with time at higher excitation.

In this Letter we report the optical studies of kinetics of the LP system under ns-long pump pulses and discover for the first time the strong hysteresis effects in the kinetics of the optical response of the pumped as well as of the scattered MC polaritons, thus directly demonstrating the behavior, predicted within the DSO OPO model [9, 11, 17].

The MC structure has been grown by a metal or-

ganic vapor phase epitaxy. The Bragg reflectors are composed of 17 (20) repeats of $\lambda/4$ $\text{Al}_{0.13}\text{Ga}_{0.87}\text{As}/\text{AlAs}$ layers in the top (bottom) mirrors. The $3/2\lambda$ GaAs cavity contains six 10-nm thick $\text{In}_{0.06}\text{Ga}_{0.94}\text{As}/\text{GaAs}$ quantum wells (QWs). The Rabi splitting is $\Omega \sim 6$ meV. A gradual variation of an active layer thickness along the sample provides a change in the photon mode energy E_C and, accordingly, in the detuning Δ between the exciton $\hbar\omega_X(\mathbf{k}=0)$ and photon $\hbar\omega_C(\mathbf{k}=0)$ mode energies. Experiments have been carried out on several spots of the same sample with Δ in the range from -1.5 to -2 meV.

The sample was placed into an optical cryostat with controlled temperature. A pulsed Ti-sapphire laser with pulse duration of ~ 1 ns, line full width at half maximum (FWHM) of ~ 0.7 meV, and pulse repetition of 5 kHz has been used for the excitation of the MC at the angle 14° relative to the cavity normal. The pump beam has been focused onto a spot with diameter of $100 \mu\text{m}$. The kinetics of angular distribution of PL signal $I(\mathbf{k}, t)$ from the MC has been detected in a wide solid angle around the cavity normal by the streak camera with spectral, angular, and time resolution of 0.28 meV, 1° , and 70 ps, respectively. The transmission signal $I_{\text{tr}}(\mathbf{k}_p, t)$ has been detected with the same streak camera.

The pump pulse profile $I_P(t)$ is shown in Fig. 1a (dashed curve). The magnitude of $I_P(t)$ determines the intensity of the external electric field outside the MC $|E_{\text{ext}}(t, \mathbf{k}_p)|^2 \propto I_P(t)$. The intensity builds up during the first 100 ps and then decreases monotonically (by about 3 times to $t = 1$ ns). The pulses with a circular (σ^+) polarization and a spectral FWHM of ~ 0.7 meV excite the MC with $\Delta = -2$ meV about 0.5 meV above the LP dispersion branch at $\mathbf{k}_p = (k_{px}, k_{py}) = (1.96, 0) \mu\text{m}^{-1}$. Figure 1b shows the recorded kinetics of MC emission normal to its plane, $I(\mathbf{k} = 0, t)$. The spectra are recorded in the σ^+ polarization. The emission in σ^- is about two orders of magnitude smaller.

The MC emission $I(\mathbf{k} = 0, t)$ is proportional to $|E_{\text{QW}}(\mathbf{k} = 0, t)|^2$, the intensity of the $\mathbf{k} = 0$ harmonic of the electric field on QW *inside* MC. Figure 1b clearly shows that $I(0, t)$ and thus the time dependence of $|E_{\text{QW}}(0, t)|^2$ differs significantly from the exciting pulse shape. At low $P = 11.5 \text{ kW/cm}^2$, the signal reaches its maximum only slightly later (by ~ 50 ps) than the pumping pulse and then decreases quickly, by one order of magnitude at $t \sim 0.35$ ns when the pump intensity is still about 60% of the maximum. At $P > 15.5 \text{ kW/cm}^2$, the signal behavior changes drastically. After its marked decrease (together with the pump) in the range of $t = 0.2 - 0.35$ ns the signal starts to grow and reaches the second maximum at $t \sim 0.85$ ns already at the excitation pulse fall off. The intensity of this maximum grows by more than two orders of magnitude in the range of P between 14.9 and 17.2 kW/cm^2 , i.e., threshold-like.

The recorded time dependences of the MC transmission at the pump angle $I_{\text{tr}}(\mathbf{k}_p, t)$ are shown in Fig. 1a

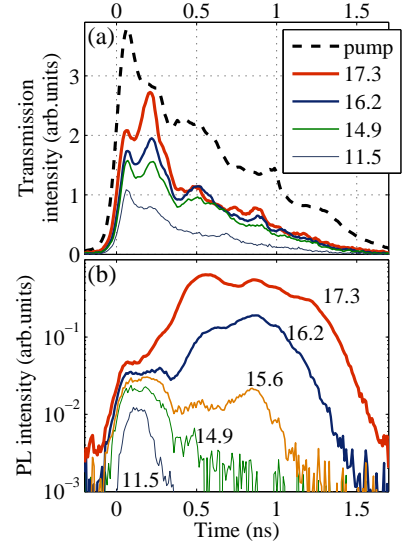


FIG. 1: (Color online) (a) Time dependences of the pump pulse $I_P(\mathbf{k}_p, t)$ and of the transmission $I_{\text{tr}}(\mathbf{k} = \mathbf{k}_p, t)$ at different excitation densities. (b) Kinetics of the LP emission intensity $I(\mathbf{k} = 0, t)$ at different excitation densities. Numbers show the peak pump intensity P in kW/cm^2 .

(solid curves). $I_{\text{tr}}(\mathbf{k}_p, t)$ is proportional to the intensity of the $\mathbf{k} = \mathbf{k}_p$ harmonic of the QW electric field $|E_{\text{QW}}(\mathbf{k}_p, t)|^2$ inside MC. Again we see clearly that $I_{\text{tr}}(\mathbf{k}_p, t)$ and thus $|E_{\text{QW}}(\mathbf{k}_p, t)|^2$ do not directly follow the exciting field $|E_{\text{ext}}(\mathbf{k}_p, t)|^2 \propto I_P(t)$. At $P \lesssim 11.5 \text{ kW/cm}^2$ I_{tr} and, thus, $|E_{\text{QW}}(\mathbf{k}_p, t)|^2$ is a monotonous superlinear function of $|E_{\text{ext}}(\mathbf{k}_p, t)|^2$ on both the up and down going parts of the excitation pulse, the maxima of $I_{\text{tr}}(t)$ and $I_P(t)$ and, hence, those of $|E_{\text{QW}}(\mathbf{k}_p, t)|^2$ and $|E_{\text{ext}}(\mathbf{k}_p, t)|^2$ nearly coincide with each other. However, the monotonous dependence $I_{\text{tr}}(I_P)$ becomes distorted with increasing P . Figure 1a shows that I_{tr} starts to demonstrate a narrow second peak in the range of nearly constant exciting field $|E_{\text{ext}}(\mathbf{k}_p, t)|^2$ at $t \sim 0.2$ ns: The growth of $|E_{\text{QW}}(\mathbf{k}_p, t)|^2$ starts at $t = 0.12 \pm 0.02$ ns, continues about 0.1 ns, and gives way to its sharp decrease at $t = 0.23 \pm 0.02$ ns. The duration of the increase and decrease in $|E_{\text{QW}}(\mathbf{k}_p, t)|^2$ is close to an available time resolution of our detecting system of 70 ps. The second peak of $|E_{\text{QW}}(\mathbf{k}_p, t)|^2$ grows quickly with P and shifts slightly towards the pulse onset.

Time dependences $I_P(t)$, $I(\mathbf{k} = 0, t)$, and $I_{\text{tr}}(\mathbf{k}_p = 0, t)$ in Fig. 1 can be redrawn as implicit functions $I_{\text{tr}}(I_P)$ and $I_S(I_{\text{tr}})$ presenting the dependences of the inner field $|E_{\text{QW}}(\mathbf{k} = \mathbf{k}_p)|^2$ on the exciting field $|E_{\text{ext}}(\mathbf{k} = \mathbf{k}_p)|^2$ and of the $\mathbf{k} = 0$ harmonic of the QW electric field on $|E_{\text{QW}}(\mathbf{k} = \mathbf{k}_p)|^2$, respectively, for each P . Figures 2a and b show the resulting dependences at $P = 16.2 \text{ kW/cm}^2 > P_{\text{thr}}$. Both the experimentally measured dependences of the $\mathbf{k} = \mathbf{k}_p$ electric field inside MC on the external field $E_{\text{QW}}|_{\mathbf{k}=\mathbf{k}_p}(E_{\text{ext}}|_{\mathbf{k}=\mathbf{k}_p})$ and of the $\mathbf{k} = 0$ electric QW field

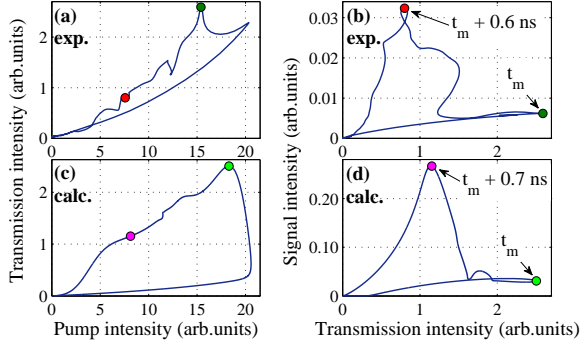


FIG. 2: (Color online) Measured (top panel) and calculated (bottom panel) dependences of transmission intensity on pump intensity and PL intensity on transmission intensity at $P = 16.2 \text{ kW/cm}^2$. Circles mark the characteristic points with maxima of transmission (at $t = t_m$) and $\mathbf{k} = 0$ emission (approximately 650 ns later).

inside MC on that at $\mathbf{k} = \mathbf{k}_p$ $E_{QW}|_{\mathbf{k}=0}(E_{QW}|\mathbf{k}_p)$ acquire jumps and hysteresis behaviour.

These experimental results find their qualitative explanation in the framework of the system of a semi-classical Gross-Pitaevskii type equation for QW excitonic polarization $\mathcal{P}(\mathbf{k}, t)$ and a Maxwell equation for $E_{QW}(\mathbf{k}, t)$ in response to the driving external field far from the MC [9, 11, 17]. According to this theoretical model, the dynamics of the stimulated parametric scattering in the planar MCs has a following scenario. Its start is initiated by a single-mode instability of the pumped mode at $\mathbf{k} = \mathbf{k}_p$, which results in the jump of $|E_{QW}(\mathbf{k}_p)|^2$ and transfers this mode into the region of its strong instability with respect to the parametric LP-LP scattering at once into a large range of \mathbf{k} . That provides an explosive growth of LP population in a wide \mathbf{k} -space region, mainly around $\mathbf{k} = 0$, on one hand, and causes the abrupt decrease in the driven mode population, on the other hand. The formation of an OPO with a three dominating macrooccupied modes with signal and idler at $\mathbf{k} = 0$ and $2\mathbf{k}_p$ occurs due to a dynamical self-organization in the multi mode scattering and takes a long – hundreds of ps – time.

The calculated dynamics of the MC optical response within the model of Refs. [9, 11, 17] at the excitation slightly above the hard excitation threshold are displayed in Fig. 2c and d. The system of Gross-Pitaevskii and Maxwell equations has been numerically solved for experimental-like time dependence of $E_{ext}(t)$. As seen from Fig. 2c,d, the model demonstrates the hysteresis in dependences of I_{tr} on I_P (panel c) and of $I(\mathbf{k} = 0)$ on I_{tr} (panel d) similar to the experimental ones. The considered model takes into account only coherent scattering processes (nondiagonal components of the LP density matrix) and neglects important scattering processes like LP-phonon or LP-free carriers. Nevertheless, it demonstrates the hysteresis in a qualitative agreement with the

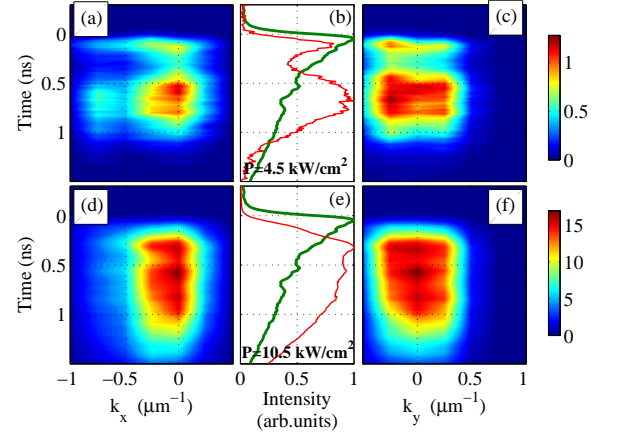


FIG. 3: (Color online) Time dependences of a k -distribution of LP emission at $P = 4.5$ (upper panels) and 10.5 (lower panels) kW/cm^2 . Left (a,d) and right (c,f) panels display the k_x dependence at $k_y = 0$ and k_y -dependence at $k_x = 0$, respectively. The thick and thin solid lines in the central panels (b,e) show, respectively, the pulse and MC emission profiles.

experiment.

The hysteresis of the dependence of I_{tr} on I_P results from the blue shift of LP eigenenergy. The increase of an overall LP population shifts the driven mode frequency towards the pump frequency, and results in increased transmissivity. Even when the pump intensity has been fallen down, the system retains considerable signal population that keeps it close to the resonance. At the same time, the hysteresis of $E_{QW}(\mathbf{k}_s \sim 0)$ vs. $I_{tr} \propto |E_{QW}(\mathbf{k}_p)|^2$ reveals a more complicated nature of the studied system. Indeed, the model does not presume any characteristic time rather than the lifetime of cavity polaritons ($\sim 3 \text{ ps}$), hence the long time of the signal developing ($\tau \sim 10^2 \text{ ps}$) might come from only the collective phenomena caused by numerous inter-mode scattering processes. Since the evolution to the “three-mode” ($\mathbf{k} = \{0, \mathbf{k}_p, 2\mathbf{k}_p\}$) state involves a lot of modes, that state appears as an essentially collective formation. Moreover, the *eventual* state differs from stable “three-mode” OPO solution even in the case of stationary pump, which may be proved by performing the stability analysis similar to that discussed in [15]. The actual stability of the three-mode pattern is maintained by the presence of numerous weak “above-condensate” modes, so the whole system occurs to be highly correlated, i.e., it demonstrates a new – dynamically self-organized – type of OPO.

To support this scenario of DSO OPO experimentally, the LP scattering dynamics in a wide range of \mathbf{k} has been measured by recording time dependences of an angle distribution of MC emission. Panels (a,d) in Fig. 3 display k_x -distribution at $k_y = 0$ whereas panels (c,f)

display k_y distribution at $k_x=0$ for the point on the MC sample with a smaller $P_{\text{thr}} \sim 3.75 \text{ kW/cm}^2$ for two excitation densities $P = 4.5$ and 10.5 kW/cm^2 , i.e., slightly and well above P_{thr} . $I_P(t)$ and $I(\mathbf{k} = 0, t)$ are given in panels (b,e). The k -distribution of the emission is symmetric in k_y direction but shows a well pronounced asymmetry in the direction of exciting pulse (k_x). The maximum emission in the very beginning of the pulse is at $k_x \sim -0.4 \mu\text{m}^{-1}$ and then during $t \sim 0.1 \text{ ns}$ it shifts to $\mathbf{k} = 0$. This behavior is well expected. The phonon-assisted scattering dominating at low LP densities cannot provide the LP relaxation to $\mathbf{k} = 0$ because of comparable magnitudes of LP life time and phonon assisted scattering time [20, 21]. The effective LP relaxation at higher densities appears due to the onset of LP-LP scatterings.

Figures 3a and c show that dynamics at $P = 4.5 \text{ kW/cm}^2$ ($\sim 20 \%$ above P_{thr}). The scattering developing after the bistable transition at $t \sim 0.4 \text{ ns}$ occurs into a wide range of wavevectors k_x between -0.7 and $+0.3 \mu\text{m}^{-1}$, k_y between $\pm 0.6 \mu\text{m}^{-1}$. With increasing time the signal intensity increases about two times and reaches its maximum at $t \sim 0.6 \text{ ns}$ without any marked narrowing in its k -distribution specific for the stimulated polariton scattering under cw excitation.

The marked narrowing of the signal in the k -space during the excitation pulse duration of $\sim 0.8 \text{ ns}$ appears at higher P . That is illustrated in Figs. 3b and d displaying the LP scattering dynamics at $P = 10.5 \text{ kW/cm}^2 \sim 3P_{\text{thr}}$. The bistable transition of the driven mode at this P occurs earlier, at $t \sim 0.1 \text{ ns}$, i.e. nearly at the pump maximum and results in a highly enhanced LP-LP scattering. The development of the stimulated signal near the band bottom in this case is followed by a monotonous narrowing of the k -distribution of the LP emission both in k_x and k_y directions. Figure 4 displaying the dependences of a FWHM of k -distribution shows that the dynamical self-organization of the parametric scattering takes a long time: the narrowing of the angle distribution takes place in the whole time range of the strong scattering signal up to $t \sim 1 \text{ ns}$. The k -distribution FWHM decreases in this time interval from ~ 1 to $0.7 \mu\text{m}^{-1}$, which is still markedly larger than the FWHM in the case of cw excitation ($\lesssim 0.3 \mu\text{m}^{-1}$). These experimental results clearly prove the DSO OPO model.

To conclude, the strong hysteresis effects in the kinetics of the pumped and scattered polariton populations have been observed for the first time in a planar semiconductor MC under a nano-second-long pulsed resonant excitation slightly above the LP branch. The hysteresis effects are explained in the model of a hard regime of the onset of parametric scattering, when the bistability of the nonlinear pumped LP mode is accompanied by the explosion-like growth of the scattered LP population and subsequent dynamical self-organization process in the open polariton system resulting in dynamically self-organized OPO.

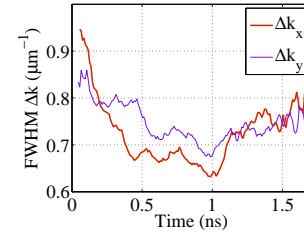


FIG. 4: (Color online) Recorded kinetics of a FWHM of k -distribution of LP emission Δk_x ($k_y = 0$) and Δk_y ($k_x = 0$) at $P = 16.2 \text{ kW/cm}^2$.

We thank M. S. Skolnick for rendered samples. This work was supported by the Russian Foundation for Basic Research, the Russian Academy of Sciences and the ANR Chair of Excellence Program.

-
- [1] R. M. Stevenson, V. N. Astratov, M. S. Skolnick, D. M. Whittaker, M. Emam-Ismael, A. I. Tartakovskii, P. G. Savvidis, J. J. Baumberg, and J. S. Roberts, *Phys. Rev. Lett.* **85**, 3680 (2000).
 - [2] A. I. Tartakovskii, D. N. Krizhanovskii, and V. D. Kulakovskii, *Phys. Rev. B* **62**, R13298 (2000).
 - [3] J. J. Baumberg, P. G. Savvidis, R. M. Stevenson, A. I. Tartakovskii, M. S. Skolnick, D. M. Whittaker, and J. S. Roberts, *Phys. Rev. B* **62**, R16247 (2000).
 - [4] C. Ciuti, P. Schwendimann, and A. Quattropani, *Phys. Rev. B* **63**, 041303 (2001).
 - [5] D. M. Whittaker, *Phys. Rev. B* **63**, 193305 (2001).
 - [6] P. G. Savvidis, C. Ciuti, J. J. Baumberg, D. M. Whittaker, M. S. Skolnick, and J. S. Roberts, *Phys. Rev. B* **64**, 075311 (2001).
 - [7] V. D. Kulakovskii, A. I. Tartakovskii, D. N. Krizhanovskii, N. A. Gippius, M. S. Skolnick, and J. S. Roberts, *Nanotechnology* **12**, 475 (2001).
 - [8] R. Butte, M. S. Skolnick, D. M. Whittaker, D. Bajoni, and J. S. Roberts, *Phys. Rev. B* **68**, 115325 (2003).
 - [9] N. A. Gippius, S. G. Tikhodeev, V. D. Kulakovskii, D. N. Krizhanovskii, and A. I. Tartakovskii, *Europhys. Lett.* **67**, 997 (2004).
 - [10] V. D. Kulakovskii, D. N. Krizhanovskii, A. I. Tartakovskii, N. A. Gippius, and S. G. Tikhodeev, *Physics – Uspekhi* **46**, 967 (2003), [*Uspekhi Fiz. Nauk* **173**, 995 (2003)].
 - [11] N. A. Gippius and S. G. Tikhodeev, *J. Phys.: Condens. Matter* **16**, S3653 (2004).
 - [12] N. A. Gippius, S. G. Tikhodeev, L. V. Keldysh, and V. D. Kulakovskii, *Physics – Uspekhi* **48**, 306 (2005) [*Uspekhi Fiz. Nauk* **175**, 327 (2005)].
 - [13] A. Baas, J. P. Karr, H. Eleuch, and E. Giacobino, *Phys. Rev. A* **69**, 023809 (2004).
 - [14] A. Baas, J.-P. Karr, M. Romanelli, A. Bramati, and E. Giacobino, *Phys. Rev. B* **70**, 161307(R) (2004).
 - [15] D. M. Whittaker, *Phys. Rev. B* **71**, 115301 (2005).
 - [16] M. Wouters and I. Carusotto, *Phys. Rev. B* **75**, 075332 (2007).

- [17] S. S. Gavrilov, N. A. Gippius, V. D. Kulakovskii, and S. G. Tikhodeev, *Zh. Eksp. Teor. Fiz.* **131**, 819 (2007), [*JETP* **104**, 715 (2007)].
- [18] W. Langbein, *Phys. Rev. B* **70**, 205301 (2004).
- [19] D. N. Krizhanovskii, S. S. Gavrilov, A. P. D. Love, D. Sanvitto, N. A. Gippius, S. G. Tikhodeev, V. D. Kulakovskii, D. M. Whittaker, M. S. Skolnick, and J. S. Roberts, submitted (2007).
- [20] J. Bloch and J. Y. Marzin, *Phys. Rev. B* **56**, 2103 (1997).
- [21] F. Tassone, C. Piermarocchi, V. Savona, A. Quattropani, and P. Schwendimann, *Phys. Rev. B* **56**, 7554 (1997).